New Regressors for the Direct Identification of Tire Deformation in Road Vehicles Via "In-Tire" Accelerometers

Sergio M. Savaresi, *Member, IEEE*, Mara Tanelli, *Member, IEEE*, Peter Langthaler, and Luigi Del Re

***Abstract*—The interaction between the tire and the road is crucial for determining the dynamic behavior of a road vehicle, and the road–tire contact forces are key variables in the design of traction, braking, and stability control systems. Traditionally, road–tire contact forces are indirectly estimated from vehicle-dynamics measurements (chassis accelerations, yaw-roll rates, suspension deflections, etc.). The emerging of the "smart-tire" concept (tire with embedded sensors and digital-computing capability) has made possible, in principle, a more direct estimation of contact forces. In this field—still in its infancy—the main open problems are the choice of the sensor(s) and the choice of the regressor(s) to be used for force estimation. The objective of this work is to present a new sensor–regressor choice, and to provide some preliminary experimental results, which confirm the validity of this choice. The idea is to use a wheel encoder and an accelerometer mounted directly in the tire. The measurement of the in-tire acceleration is transmitted through a wireless channel. The key innovative concept is to use the phase shift between the wheel encoder and the pulse-like signals provided by the accelerometer as the main regressor for force estimation.**

***Index Terms*—Road vehicles, road vehicle control, road vehicle identification, identification, signal processing.**

I. Introduction

THE tire is probably the single component, which mostly affects the dynamic behavior and performance of a road vehicle. As a matter of fact, the largest part of the external forces acting on the vehicle is transmitted through the road–tire contact patch. The developments in the tire materials, structure, and manufacturing techniques have been enormous in the last decades. However, the tire has essentially remained a "passive" object.

In the last few years, a new trend has emerged: the measurement and low-bandwidth transmission of the tire pressure is an industrial reality (tire pressure monitoring system (TPMS) systems; see, e.g., [9]), and new in-tire sensors and electronics are currently under research [12], [15]. This trend is mainly driven by information and communication technology (ICT) methods and devices, and represents a small revolution in tire manufacturing. The term "smart tire" is frequently used to label this new-generation tires.

In the field of smart tires, today, the main challenge is the direct real-time estimation of the road–tire contact forces via "in-tire" sensors. This research is still in its infancy, and a number of nontrivial issues are still open. Among others are the choice of in-tire sensors, the in-tire preprocessing of the signal, the wireless transmission, the postprocessing, the regressor choice, the estimation algorithm, etc. The problem becomes even more complicated with technological and industrial issues like durability, cost, and energy consumption of the in-tire electronic devices.

The great interest in a smart tire capable of providing a real-time estimation of the road–tire contact forces is easily explained by its huge potential benefits: the direct measurement of road–tire contact forces can stimulate the development of a new generation of traction, braking, and stability control systems [3], [6], [10], [14], [20]–[26]. Hence, the impact of this new tire technology on the overall vehicle dynamic performance (in terms of safety, driving satisfaction, energy consumption, etc.) can be potentially very large and motivates the research in this field. The main motivation of this research area is "control oriented," because the contact force estimation is not an intrinsic or "final" objective, but it is functional to control-related objectives, like fast closed-loop stability control systems [antilock breaking system (ABS) and electronic stability system (ESC)], roll-pitch control performed by active or semiactive suspensions and roll-bars, fault detection, and sensor reconfiguration, etc., (see, e.g., [23]–[25]).

As already said, the direct estimation of contact forces via "smart tire" is still in its early stages: no commercial products are available on the market, but many research groups are exploring and testing different solutions. The two key issues (strictly interleaved), still open, can be summarized as follows.

- Which is the best tire-embedded sensor choice?
- Given the sensor-configuration, which is the best set of regressors to be used for force estimation?

The purpose of this brief is to present a possible solution to these two open issues, and to provide some experimental results as a preliminary validation. Given the early stage of this research field, the scope of this work is not to provide a fully tested ready-to-market technique, but to validate an idea of a "system" constituted by sensors, regressors, and algorithms. Specifically, this method has been developed having in mind the goal of estimating the road–tire vertical and longitudinal forces. The method proposed herein makes use of two sensors in each wheel:

Manuscript received October 25, 2006; revised April 30, 2007. Manuscript received in final form August 30, 2007. Recommended by Associate Editor I. Haskara. This work was supported in part by the Italian Ministry for University and Research (MIUR) project "New methods for identification and adaptive control for industrial systems" and the project 22/2004 "Smart tires: tire-road friction forces estimation via signal processing of innovative sensors," within a scientific collaboration program between Italy (represented by the Politecnico di Milano, Milano, Italy) and Austria (represented by the Johannes Kepler University, Linz, Austria). This work was also supported by the Pirelli Tyres S.p.A., Milano, Italy.

S. M. Savaresi and M. Tanelli are with the Dipartimento di Elettronica e Informazione, Politecnico di Milano, 20133 Milano, Italy (e-mail: savaresi@elet.polimi.it; tanelli@elet.polimi.it).

P. Langthaler and L. del Re are with the Institute for Design and Control of Mechatronical Systems, Johannes Kepler University, 4040 Linz, Austria (e-mail: Peter.Langthaler@jku.at; Luigi.delre@jku.at).

Digital Object Identifier 10.1109/TCST.2007.912245

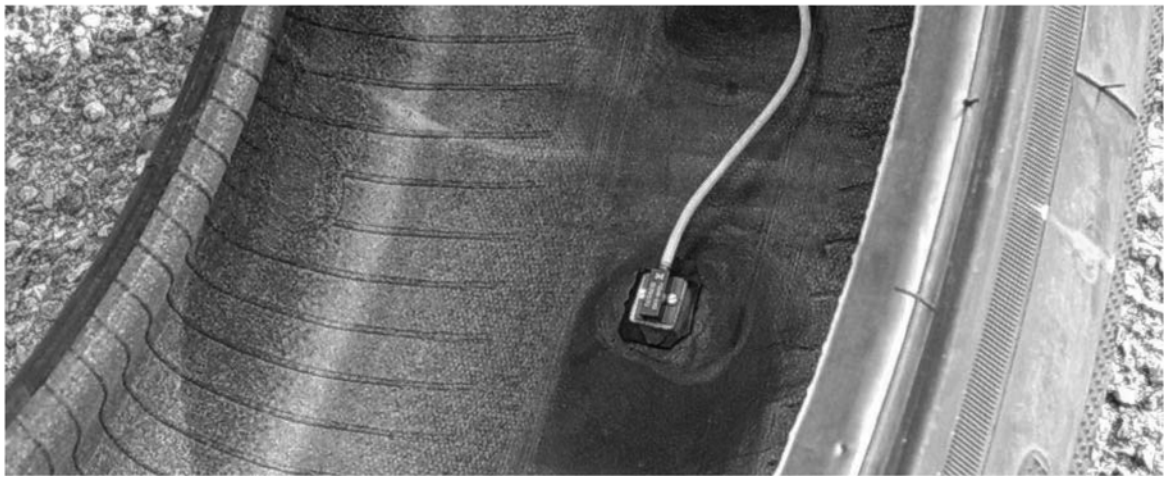

Fig. 1. Detail of the in-tire accelerometer.

- a standard wheel encoder typically used by ABS systems for the wheel-speed measurement;
- a one-axis accelerometer mounted directly in the tire, which measures the acceleration experienced by the tire in the radial direction.

The key idea of the method is to measure the phase shifts between the wheel encoder and the impulse-like signals detected by the accelerometer when it encounters and leaves the road–tire contact patch. In this brief, it will be shown that these phase shifts seem to be strongly correlated with the longitudinal and vertical tire deformation; henceforth, they could be used for force-identification purposes.

The material presented herein is the result of a set of experiments made on a real car in a simplified low-budget setting: the tests have been performed on a flat dry-asphalt surface, when driving in a straight line at low/midrange speed (0–80 km/h). Two tire pressures settings have been tested, in order to understand the sensitivity of the method with respect to this critical parameter. The results are very encouraging, and the scope of this brief is to present the key idea and the whole signal processing procedure, which represent the main contributions. The simplified setting also allows an effective description and explanation of the bulk of the method.

To the best of our knowledge, in the open scientific literature, very little has been published on the topic of direct estimation of road–tire contact forces by in-tire sensors. In this field, a recent paper by a Toyota research team [13] is worth mentioning, where an interesting method for the estimation of the so-called "extended braking stiffness" is described. Most of the current research activity on this topic has not been published yet; it is only roughly described in industrial patents (see, e.g., [5] and [16]) or in oral presentations (see, e.g., [12]). Instead, the general topic of contact-force estimation (not directly related to the "smart-tire" concept) has been widely studied in the last decade. Some relevant references are, e.g., [4], [7], [8], [18], and [19].

The outline of this brief is as follows. In Section II, the experimental setup and the measured signals are briefly described. In Section III, the main idea of the sensor/regressor choice is concisely presented. Section IV is devoted to the detailed presentation of the signal processing. In Section V, some final identification results are presented and discussed. This brief ends with some conclusive remarks.

II. Experimental Setup

All the material presented herein has been developed with a simple experimental setup. The test car is a rear-wheel-driven BMW 320 d (E46) with manual transmission, equipped with the following set of sensors.

- Four inductive 48-steps Hall-effect encoders, which measure the wheel rotational speed [they are standard ABS wheel encoders originally installed by the original equipment manufacturer (OEM)]. The output of these sensors is a sinusoidal-like signal, whose frequency is proportional to the rotational wheel speed ω.
- One one-axis, ± 500 g piezoresistive low-mass linear accelerometer (ENDEVCO® 7264B), mounted (glued) inside the tire (Fig. 1), which measures the in-tire radial acceleration tire; the accelerometer has been installed alternatively on the front-left tire and on the rear-left tire. Its bandwidth is about 3 kHz.

The wireless data transmission of the in-tire acceleration signal is made via a Datatel™ (Langenhagen, Germany) telemetry system. The transmitter and its battery are mounted on the wheel rim. The receiver antenna is placed on the car roof; the acquisition of the sensor signals is made by a DSpace Autobox™ (Wixom, MI) acquisition system. All the signals are sampled at 10 kHz, with a 16-bit resolution.

The driving tests were all made on the same road surface, a high-grip flat dry-asphalt road, in order to eliminate the dependency of the results on the road conditions. Two main types of tests have been done:

- quasi-static tests: very slow decelerations and accelerations (with no gear shifts) in the range 10–25 m/s;
- dynamic tests: strong braking and acceleration maneuvers, interleaved with constant-speed intervals.

All the test are performed on a straight road. Two tire-pressure conditions have been tested: 2.0 bar (nominal condition) and 1.6 bar (low-pressure condition).

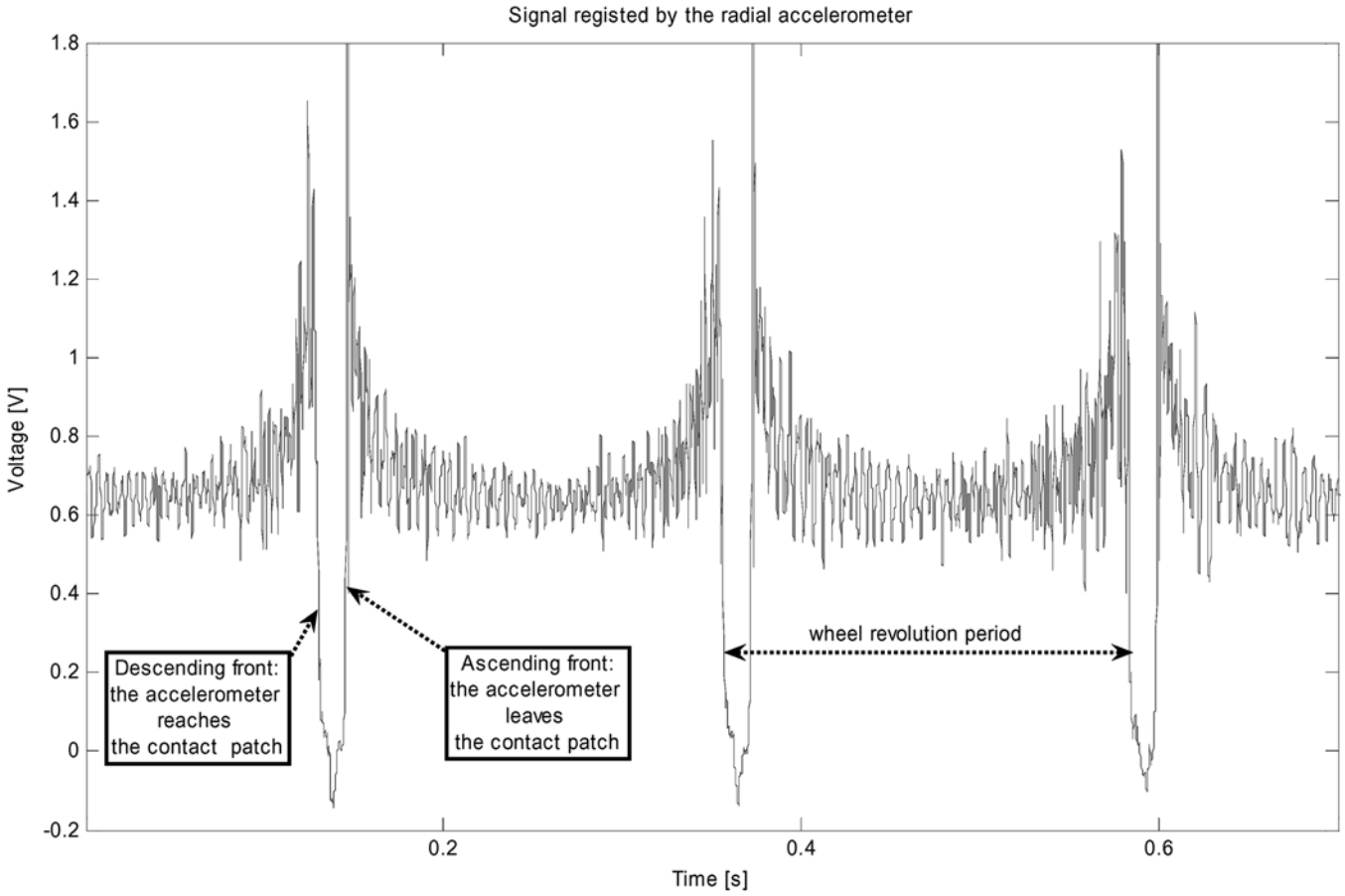

Fig. 2. Raw signal detected by the radial in-tire accelerometer.

III. Main Concept

Consider the signal detected by the in-tire accelerometer. It measures the instantaneous acceleration experienced by the tire at the installation point, in the radial direction. An example of this signal (the raw signal, without any kind of preprocessing) over a 0.7-s time window is displayed in Fig. 2. The analysis of this signal reveals that the radial acceleration is roughly constant over a short-time window (it is the centripetal acceleration, proportional to the wheel speed), but when the accelerometer passes through the contact patch the acceleration is characterized by two impulse-like signals; this twin spike is obviously repeated every wheel revolution.

The two main "fronts" of the acceleration signal around the contact patch (the first is descending and the second is ascending) can be used to detect the time instants when the accelerometer reaches and leaves the contact patch, respectively.

The key idea proposed herein is to estimate the vertical and the longitudinal force acting on the tire by using the following regressor: the phase shift between the wheel hub and the tire (computed from the wheel-speed sensor and the two acceleration impulses).

In order to get a more visual description of this idea, consider Fig. 3(a), where a schematic picture of a wheel and its contact patch is displayed. If we consider the two acceleration spikes, and their absolute position in the angular reference frame α given by wheel encoder (which is not subject to elastic deformation), at each wheel revolution three quantities can be computed:

- the angular position α_1 of the initial position of the contact patch;
- the angular position α_2 of the final position of the contact patch;
- the length $\Delta\phi = \alpha_2 - \alpha_1$ of the contact patch.

In Fig. 3(b) and (c), the phase-shift phenomenon is pictorially described. More specifically, the following can be said.

- Due to the elastic properties of the tire in the radial direction [1], [2], [14], the vertical road–tire contact force F_z is assumed to be strictly correlated with the width $\Delta\phi = \alpha_2 - \alpha_1$ of the contact patch [Fig. 3(b)]; the idea hence is to use the measured angle $\Delta\phi$ to estimate F_z: $F_z = f_z(\Delta\phi)$.
- Due to the elastic properties of the tire in the longitudinal (tangential) direction [1], [2], [14], the longitudinal road–tire contact force F_x is assumed to be strictly correlated to the phase shift of the center of the contact patch $\delta\phi = (\alpha_1 + \alpha_2)/2$ [Fig. 3(c)]; the idea is to use the measured angle $\delta\phi$ to estimate F_x: $F_x = f_x(\delta\phi)$. In particular, note that $\delta\phi$ is expected to be negative during braking, and positive during acceleration; in other words, this means that the center of the contact patch is assumed to rotate backward or forward (with respect to a conventional zero position), respectively. Also notice that, in general, the real

Fig. 3. (a) Schematic representation of a wheel and its contact patch. (b) Effect of a vertical force variation. (c) Effect of a longitudinal force variation.

center of the contact patch is not perpendicular to the wheel hub. This means that $\delta\phi = (\alpha_1 + \alpha_2)/2$ is a "conventional" center of the contact patch. This however does not affect the estimation procedure, because the procedure is insensitive to the "conventional" choice of the contact patch center.

The theoretical background of this idea can be found, e.g., in [11] and [14, Ch. 3]. In these works, the vertical and longitudinal elastic behavior of the tire, during acceleration and braking, is described. More specifically, in [14, Ch. 3], the so-called "tire brush model" is presented and discussed.

It is well known, however, that mathematical modeling of road–tire contact forces is a very challenging and elusive problem, and physical or semiphysical models can only provide a general explanation of the main phenomenon; a very accurate

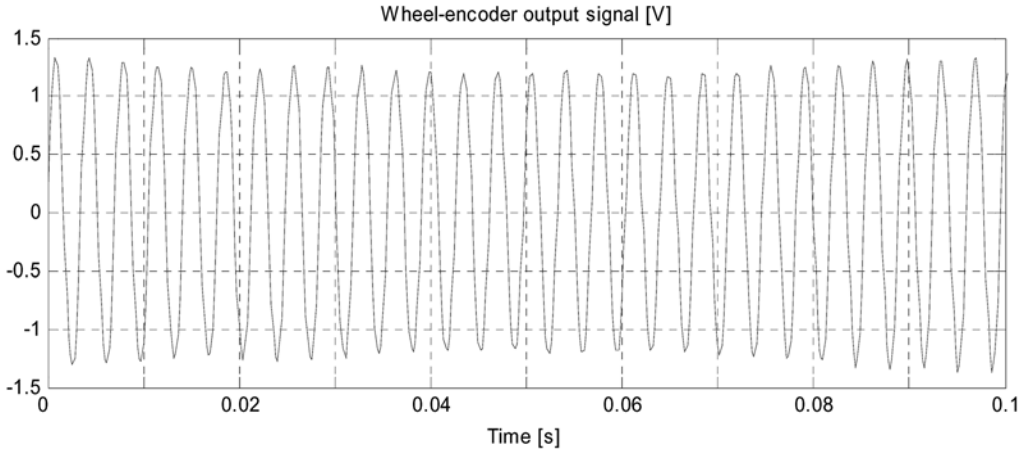

Fig. 4. Example of the measured wheel-encoder signal.

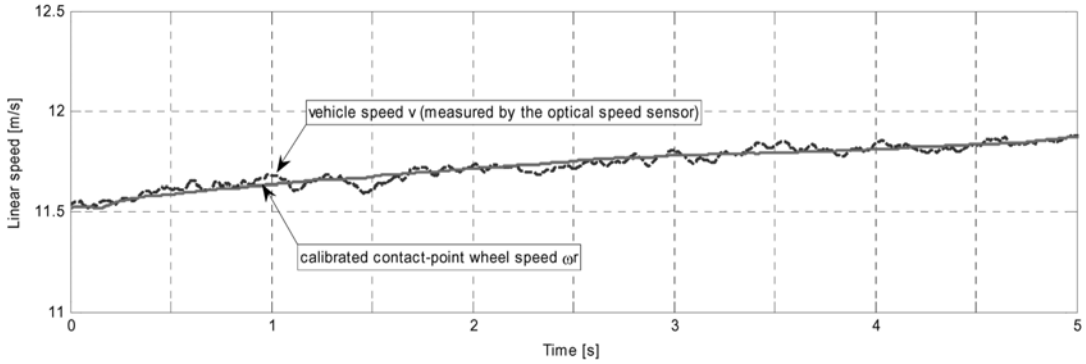

Fig. 5. Example of calibrated wheel speed at the contact point.

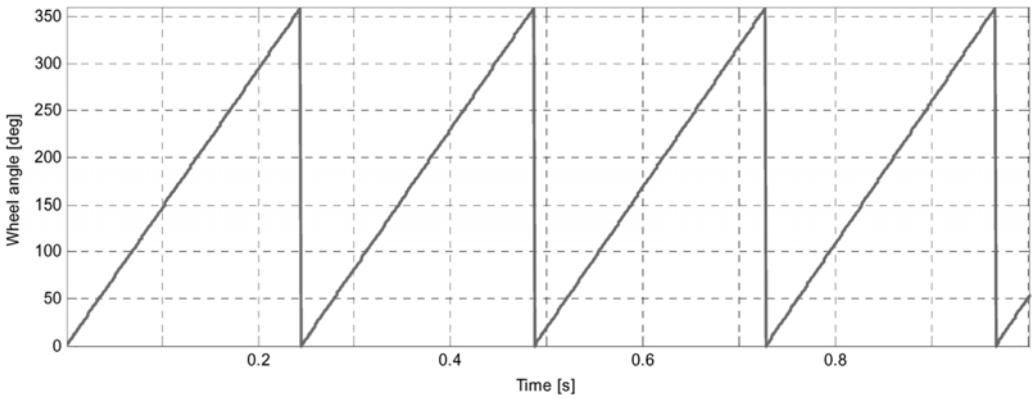

Fig. 6. Example of the estimated angular position α of the wheel from the wheel encoder.

fitting between models and data can usually be obtained only with a genuine black-box approach. The contribution of this work is to show how the longitudinal and vertical elastic behavior of the tire can be exploited for run-time contact-force estimation, using a simple (and cheap) configuration of sensors.

The goal of the rest of this brief is to corroborate with experimental evidence the above idea and assumptions; this is far from being trivial, since the phase shifts are expected to be small, and a lot of spurious effects must be considered and removed.

IV. Signal Processing

The whole method proposed in this brief is based on the measurement of two signals for each wheel: the wheel rotational speed ω and the radial acceleration a_{tire} experienced by a point in the tire. The digital signal processing of these two signals is now described.

A. Wheel-Encoder Signal

The wheel encoder is the standard 48-steps encoder used by the ABS and ESC control systems, originally installed by the

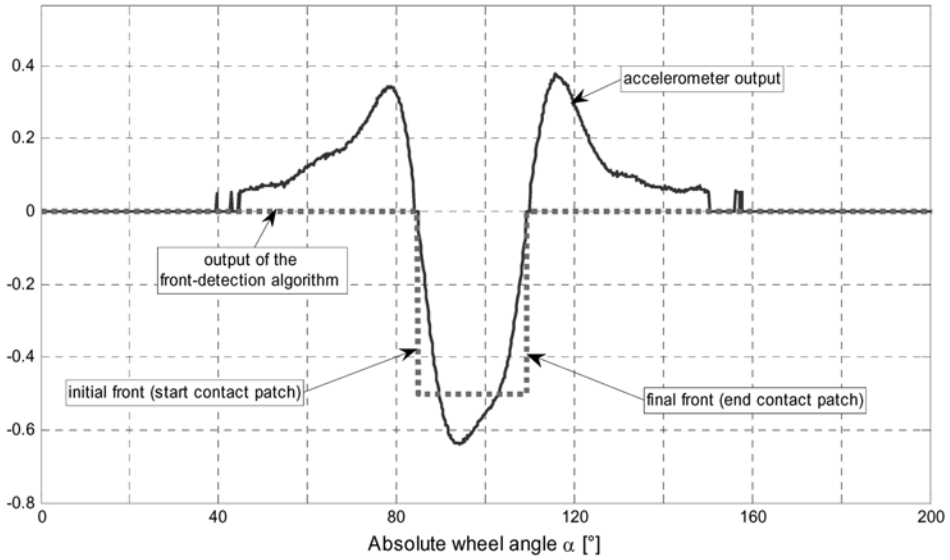

Fig. 7. Example of output of the front-detection algorithm.

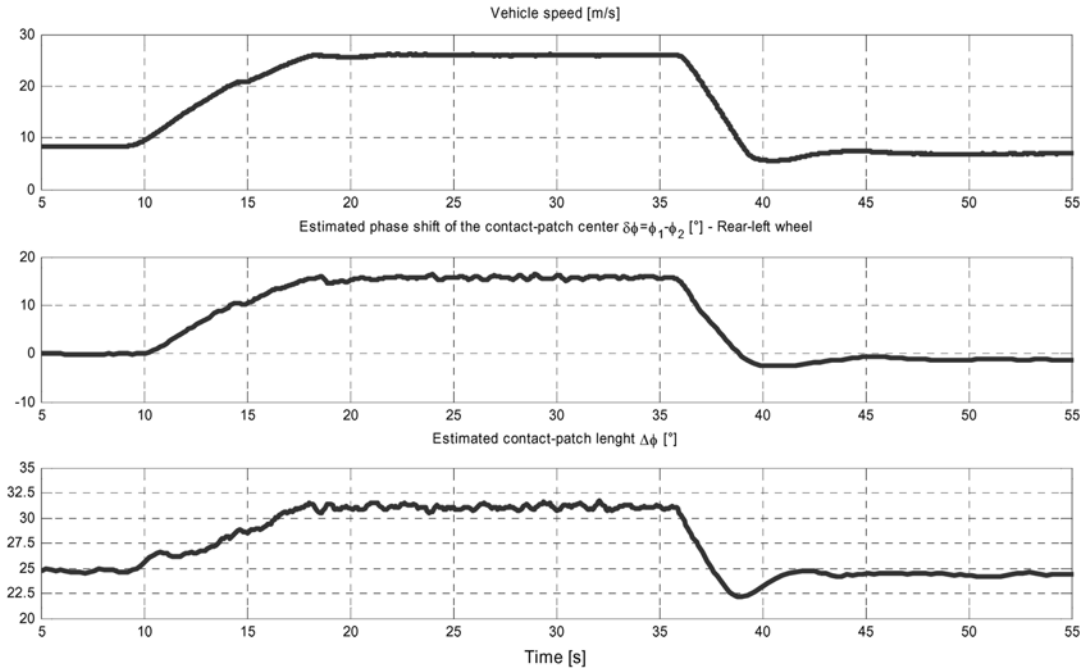

Fig. 8. Example of a complete dynamic test. The phase shift and width of the contact patch are referred to the rear-left wheel.

OEM. The original signal coming from the encoder is a sinusoidal-like voltage signal. An example of this signal is displayed in Fig. 4, over a time window of 100 ms. In order to estimate the wheel rotational speed, the wheel-encoder signal must be passed through a high-accuracy frequency tracker, since the wheel speed is linearly proportional to the instantaneous frequency of the sinusoidal signal. Many digital signal processing techniques can be used. In this work, a mix of the techniques described in [17] and [20] has been resorted to, complemented with a windowing technique, which corresponds to low-pass filtering at a cutoff frequency of 20 Hz. These techniques are based on digital notch filters. They are well known and easy to be implemented online.

In order to compute the linear speed of the contact point v_c, the estimated wheel rotational speed ω must be multiplied by the wheel effective radius r: $v_c = r\omega$. The accurate estimate of the quasi-static effective radius has been done using the measurement of the vehicle speed v provided by the optical speed sensor. In Fig. 5, an example of the calibrated v_c signal (for the front-left wheel) is displayed. Notice that the estimation of the radius is not particularly critical, because the proposed regressors are based on phase shifts, which are not strongly correlated with the actual wheel radius. In the method we propose, the wheel speed is only used to remove speed-dependent trends. Henceforth, an accurate calibration of the wheel effective radius is not strictly mandatory.

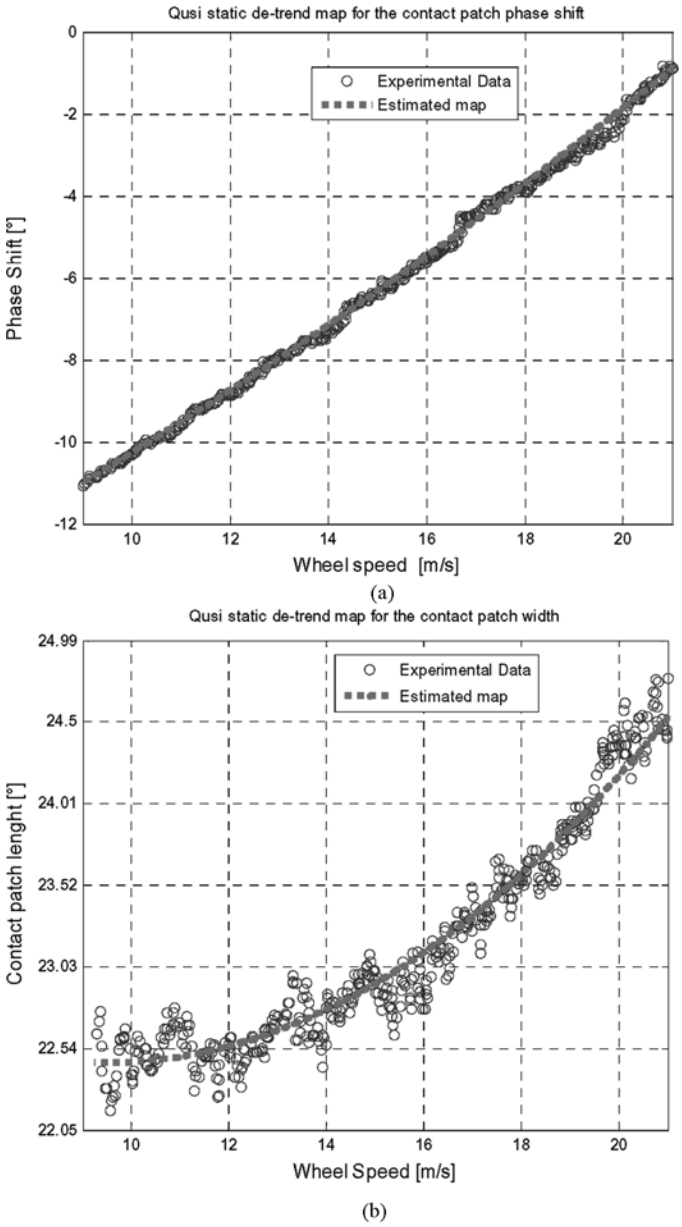

Fig. 9. Quasi-static maps of the (a) phase shift and (b) contact patch length as functions of wheel speed.

The main step of the preprocessing of the wheel-encoder signal is to estimate the instantaneous angular position α of the wheel. This estimation is fundamental because it represents the baseline for the identification of the accelerometer-based phase shift. The basic idea for the estimation of the angular position is simply to make an incremental step counter, which resets every 48 steps (or 360°). Because in a 48-steps encoder the peak-to-peak distance of one period corresponds to 7.5° of wheel rotation, the whole sinusoidal profile of the signal (Fig. 4) must be used to improve the accuracy of the angular position. The obtained angular resolution can be estimated in about 0.1°, which is suitable for this application. An example of the estimated wheel angular position is displayed in Fig. 6.

B. In-Tire Acceleration Signal

The in-tire accelerometer is a one-axis (oriented in the radial direction), ±500 g piezoresistive low-mass linear accelerometer, glued inside the tire. The output signal is a voltage signal, characterized by a bump (or a twin impulse) around the road–tire contact patch. As already said, the main signal processing issue is to detect the time instant when each impulse takes place, namely, to detect the angular positions α_1 and α_2 of the two fronts (one descending and one ascending) of the bump. In Fig. 7, an example of the output of the front-detection algorithm is displayed (dashed line). The front-detection algorithm implemented herein essentially performs a simple zero-crossing search in the neighborhood of the two main fronts; the zero-crossing algorithm is applied to the normalized and detrended signal. Note that in Fig. 7 the signals are plotted as a function of the wheel absolute angular position α, not as a function of time. The replacement of the time domain with the phase domain is a key step, which allows the removal of most of the dependency of the phase shift from the wheel rotational frequency.

Starting from α_1 and α_2, the estimation of the width of the contact patch $\Delta\phi$ is straightforward: $\Delta\phi = \alpha_2 - \alpha_1$.

For the computation of the phase shift of the midpoint of the contact patch $\delta\phi$, the following procedure was used. The first part of every test drive is always characterized by a low-constant-speed (about 10 m/s) condition. It is conventionally assumed that the phase shift in that condition is zero, namely, $\delta\phi = (\alpha_1 + \alpha_2)/2 + \Omega_0 = 0$. The calibration offset Ω_0 is then added to the absolute angular position of the wheel for the entire experiment. In other words, it is assumed that at the beginning of each experiment the phase shift is zero, and all the phase shifts of the rest of the experiment are referred to that conventional zero condition. As already remarked, the choice of this conventional "zero" Ω_0 does not affect the quality of the estimation and does not depend on speed or road conditions.

C. Remark (on the Number and Precision of Sensors)

In the sensor configuration discussed previously, a standard 48-steps ABS wheel encoder and a single embedded accelerometer have been used. This sensor configuration is the simplest and the cheapest, but it may have some limitations. The most evident is the fact that the phase-shift information is refreshed only once per revolution. This refresh time can be too long for the control of fast dynamics (ABS or ESC). On the other hand, a low-resolution encoder obviously limits the resolution of the angle estimation and the signal-to-noise ratio (SNR) of the estimated angle. Clearly, these limits can be easily removed by adopting a different sensor configuration, with an array of accelerometers and a more sophisticated angle sensor (e.g., the magnetic sensors used in recent ABS/ESC applications, which can provide a continuous position signal). As already stressed, the detailed analysis of these extended sensor setups is out of the scope of this work.

The results of the previously described preprocessing of the two main signals can be appreciated in Fig. 8, where the vehicle speed, the phase shift of the midpoint of the contact patch $\delta\phi$, and the contact-patch width $\Delta\phi$ are displayed, for a 1-min-long dynamic experiment. From the behavior of the vehicle speed, note that experiment is constituted by five main parts: a first part of constant low speed, an acceleration, a new long constant-

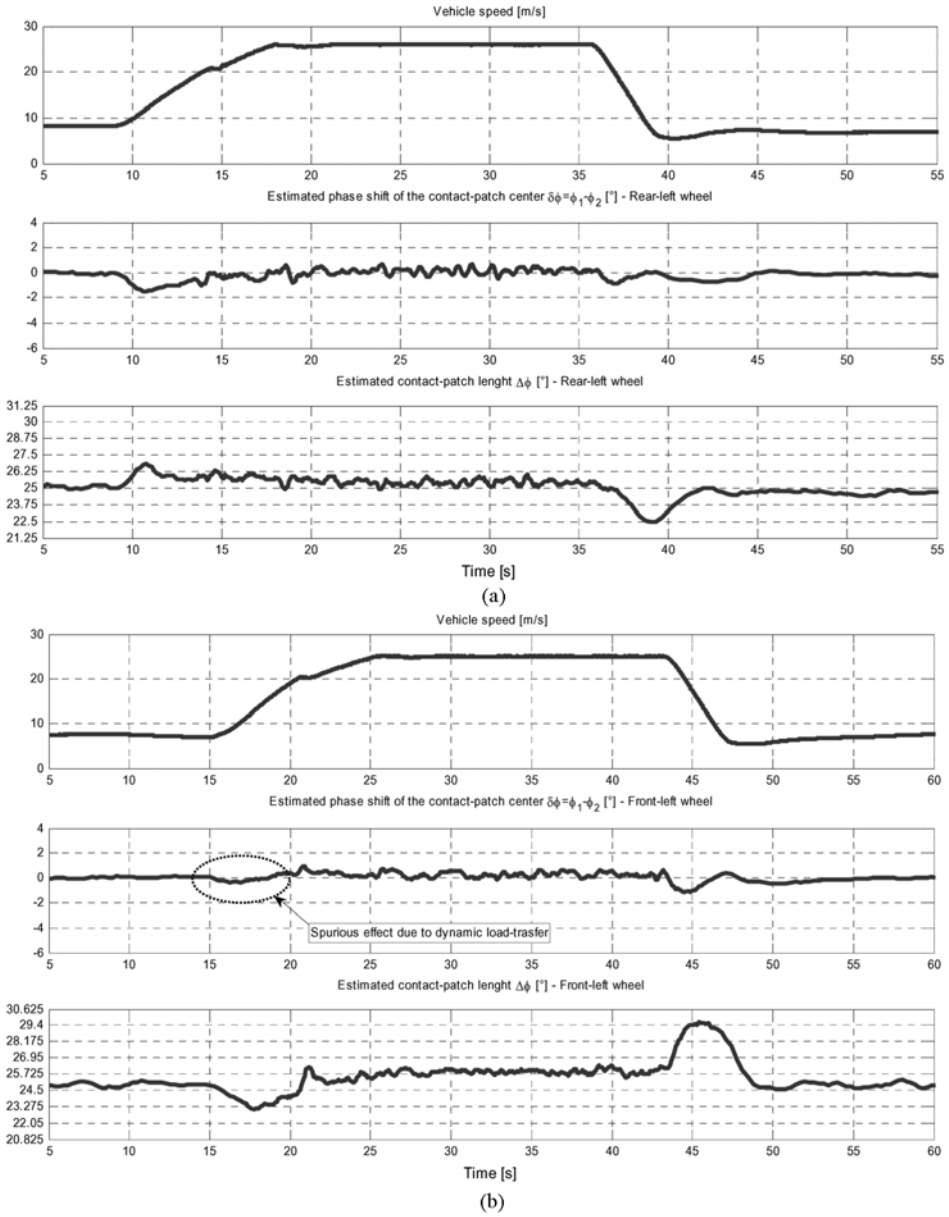

Fig. 10. (a) Example of a complete dynamic experiment. Rear-left wheel; nominal pressure. (b) Example of a complete dynamic experiment. Front-left wheel; nominal pressure.

speed window, a strong braking maneuver, and a final constant low-speed condition.

By inspecting the estimated $\delta\phi$ and $\Delta\phi$ in Fig. 8, it is immediately apparent that their behavior is highly correlated with the vehicle speed.

Unfortunately, this speed-dependency phenomenon hides almost completely the important part of the relationships between the pair $(\delta\phi, \Delta\phi)$ and the contact forces (F_x, F_z). The removal of the speed-dependent trends in $\delta\phi$ and $\Delta\phi$ hence is mandatory. Note that this effect is not surprising, and it is mainly due to the effects of the aerodynamic forces and (at mid-low speed) of the rolling resistance.

In order to remove this spurious effect, a simple quasi-static experiment was performed: the car has been slowly accelerated (without gear shift) from 10 to 25 m/s; the same experiment has been repeated in deceleration (coasting down). Because the acceleration/deceleration ramp is extremely slow, in this experiment, the dynamic effects can be neglected.

At each wheel revolution, the pairs $(v_c, \delta\phi)$ and $(v_c, \Delta\phi)$ have been computed. The results are plotted in Fig. 9.

Because the experiment has been made in a quasi-static setting, the relationships depicted in Fig. 9 are static and can be easily fitted with 1-D nonlinear functions. In particular, both maps have been fitted with simple second-order polynomials. A unique map has been used both for the front and the rear tire. It is expected that on cars where the front and rear static loads are strongly different, two different maps (one for the front and one for the rear) should be used. Also, the estimated maps are displayed in Fig. 9.

Using the estimated maps, the speed-dependent trends have been removed from the dynamic experiments. The results are displayed in Fig. 10, for both the rear and the front wheels. Note

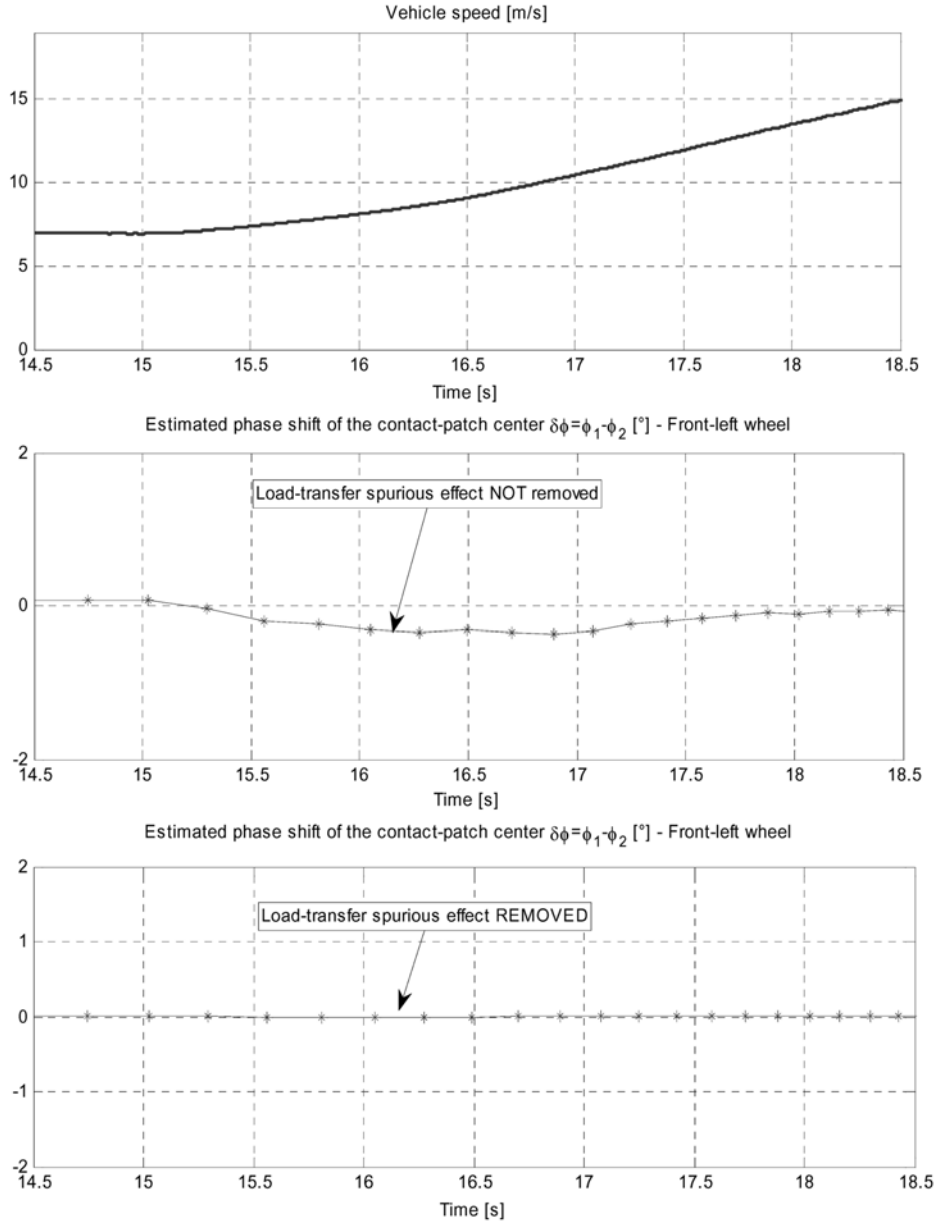

Fig. 11. Detail of the acceleration phase (front wheel) before and after the removal of the load-transfer spurious effect.

that, after the trend removal, the phase shift and the width of the contact patch have the same value (0° and 25°, respectively) in every constant-speed condition.

By carefully inspecting Fig. 10(b) (front tire), another residual spurious effect can be observed. As a matter of fact, notice that, during the acceleration phase, no significant longitudinal force F_x should be exerted to the front wheels; as a consequence, we know *a priori* that the phase shift of the contact patch on a front wheel in that condition should be zero. This condition is not perfectly met by the data displayed in Fig. 10(b) (see the dotted oval box). This phenomenon has a simple and intuitive explanation: there is a slight dependency (or "cross talk") between the phase shift and the vertical force. Henceforth, the phase shift must be subject to an additional correction as follows:

$$\delta\phi = \delta\tilde{\phi} + f_F(F_z) \tag{1}$$

where $\delta\tilde{\phi}$ is the phase shift without correction, and $f_F(F_z)$ is the correction term (to be estimated). Unfortunately, F_z is not directly known. However, because we have assumed a direct static relationship between F_z and $\Delta\phi$, we can approximate (1) with the following equation:

$$\delta\phi = \delta\tilde{\phi} + f(\Delta\phi). \tag{2}$$

For simplicity, we have assumed a linear dependency from the correction term, namely

$$\delta\phi = \delta\tilde{\phi} + k(\Delta\phi - \Delta\phi_0). \tag{3}$$

The term $(\Delta\phi - \Delta\phi_0)$ is the dynamic variation of the contact patch width ($\Delta\phi_0$ is the average value of the contact patch, at constant speed). The only unknown term in (3) is the coefficient

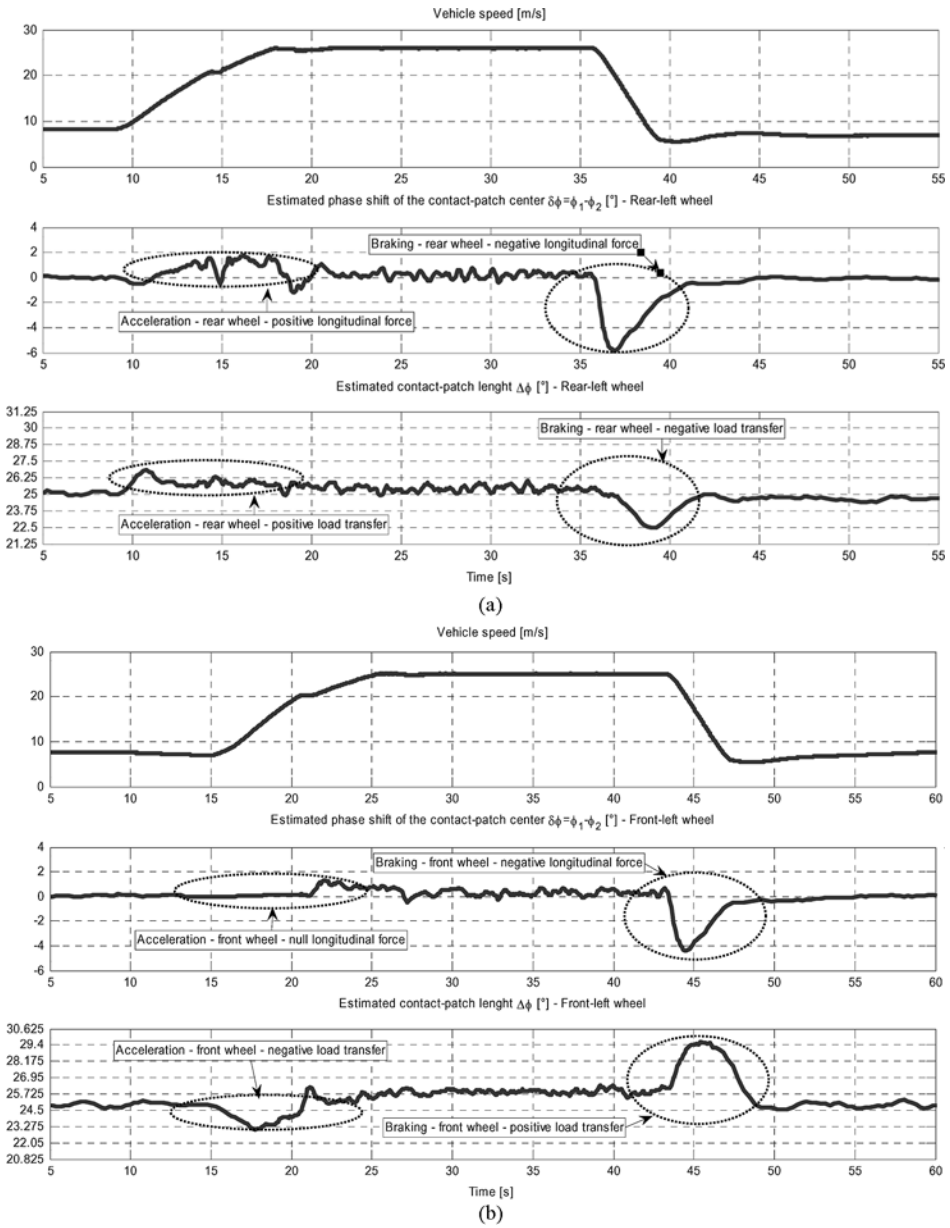

Fig. 12. (a) Example of a complete dynamic experiment. Rear-left tire; nominal tire pressure. (b) Example of a complete dynamic experiment. Front-left tire; nominal tire pressure.

k. The optimal value of k has been identified by numerical optimization from data, in order to guarantee no phase shift on the front tire during acceleration, in every working condition.

In Fig. 11, the detail of the acceleration phase for the front tire before and after the correction with (3) is shown.

Using the estimated value of k, the entire phase-shift signals of both the front and the rear wheels have been modified according to (3).

After the single (for the contact patch width) and the double (for the phase shift) trend removal, all the main spurious effects are eliminated. In Section V, the obtained final results will be presented and discussed.

V. Experimental Results

In this section, we present the final results of the phase shift and the contact patch length estimation on both front and rear wheel, measured on the dynamic test drives introduced in Section II. Two different tire pressures are tested: a nominal pressure of 2.0 bar and a reduced pressure of 1.6 bar. We recall that such results have been obtained after removing the speed-dependent trend on both the phase shift and width of the contact patch, and after eliminating the load-dependent spurious effects on the phase shift (see Section IV).

Fig. 12 shows the results for the nominal pressure, for both the front and the rear wheels. By carefully inspecting this figure, we can finally check and verify the consistency of the main idea and rationale described at the beginning of this brief. More specifically, the following observations can be made.

- **Acceleration phase—longitudinal force**. During this phase, no longitudinal force is applied at the front wheel $(F_{x(\mathrm{FRONT})} = 0)$, whereas a positive force is applied at the rear (drive) wheel $(F_{x(\mathrm{REAR})} > 0)$. Accordingly,

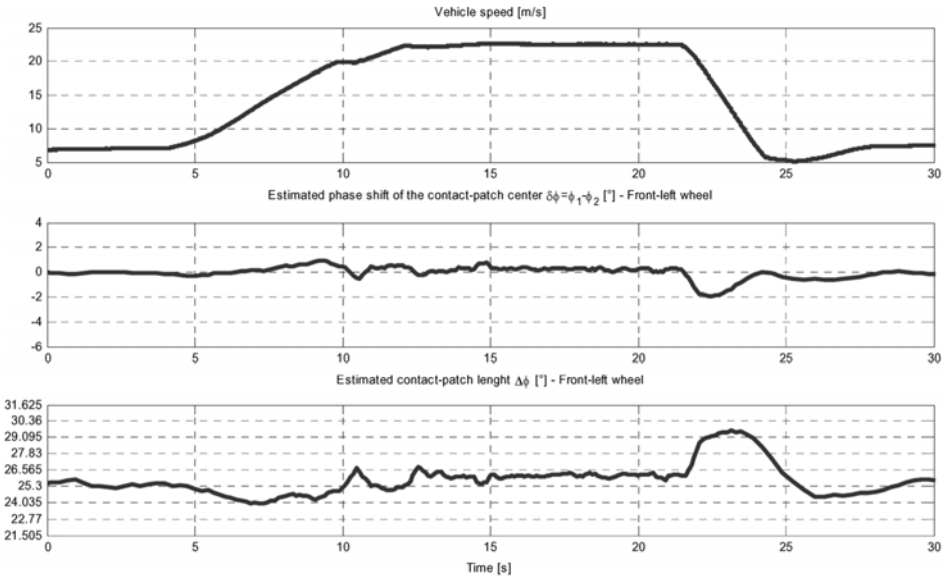

Fig. 13. Example of a complete dynamic experiment. Front-left tire; reduced tire pressure.

because we have assumed a direct monotone static relationship $F_x = f_x(\delta\phi)$ between the longitudinal force F_x and the phase shift of the contact patch $\delta\phi$, the phase shift of the front wheel should be zero $(\delta\phi_{(\mathrm{FRONT})} = 0)$, whereas the phase shift at the rear wheel should be positive $(\delta\phi_{(\mathrm{REAR})} > 0)$. From Fig. 12, it is easy to see that both these conditions are met.

- **Acceleration phase—vertical force**. During this phase, the front wheel should experience a decrease of the vertical force ($F_{z(\mathrm{FRONT})} < \bar{F}_{z(\mathrm{FRONT})}$, where $\bar{F}_{z(\mathrm{FRONT})}$ is the static load at the front wheel), whereas the vertical force at the rear wheel should increase ($F_{z(\mathrm{REAR})} > \bar{F}_{z(\mathrm{REAR})}$, where $\bar{F}_{z(\mathrm{REAR})}$ is the static load at the rear wheel). Accordingly, since we have assumed a direct monotone static relationship $F_z = f_z(\Delta\phi)$ between the longitudinal force F_z and the width of the contact patch $\Delta\phi$, the width at the front wheel should decrease $(\Delta\phi_{(\mathrm{FRONT})} < \Delta\phi_0)$, whereas the width at the rear wheel should increase $(\Delta\phi_{(\mathrm{REAR})} > \Delta\phi_0)$. From Fig. 12, it is easy to see that also both these conditions are met.
- **Braking phase—longitudinal force**. During this phase, a negative longitudinal force is applied at both wheels $(F_{x(\mathrm{FRONT})} < 0, F_{x(\mathrm{REAR})} < 0)$. Accordingly, we expect that $\delta\phi_{(\mathrm{REAR})} < 0$ and $\delta\phi_{(\mathrm{FRONT})} < 0$. From Fig. 12, it is easy to see that these conditions are met.
- **Braking phase—vertical force**. During this phase, the front wheel should experience an increase of the vertical force $(F_{z(\mathrm{FRONT})} > \bar{F}_{z(\mathrm{FRONT})})$, whereas the vertical force at the rear wheel should decrease $(F_{z(\mathrm{REAR})} < \bar{F}_{z(\mathrm{REAR})})$. Accordingly, we expect that $\Delta\phi_{(\mathrm{FRONT})} > \Delta\phi_0$ and $\Delta\phi_{(\mathrm{REAR})} < \Delta\phi_0$. From Fig. 12, it is easy to see that also both these conditions are met.

Regarding the signals displayed in Fig. 12, notice that the noise on the estimated phase shift and contact-patch length is higher in the time window 25–40 s than in the time window 5–15 s. This is simply due to the change of the forward speed.

In Fig. 13, the results of the experiments performed with low-pressure tires are displayed. Notice that the results displayed in Fig. 13 are obtained without recalibration: they have been computed using the same preprocessing and calibrations used for the 2.0-bar case, in order to test the robustness of the method. All the considerations made in the nominal pressure case still hold; this fact is encouraging since the method shows a good robustness with respect to pressure variations.

By carefully comparing the results at nominal and low pressures, one can notice that, as expected, the contact patch width is slightly larger in the case of low-pressure tires; the variations in the phase shift and contact patch length instead are very similar to the nominal pressure setting.

The previous results have fully confirmed the rationale presented at the beginning of this brief (Section III), and they show that the identification method proposed here is feasible. Obviously, in order to be of practical usage, a much larger set of experiments, both on the car and on a test bench should be performed. In particular, in order to estimate the mappings $F_x = f_x(\delta\phi)$ and $F_z = f_z(\Delta\phi)$, test-rig experiments must also be done.

VI. Concluding Remarks and Future Work

In this brief, we presented an innovative approach for estimating the instantaneous vertical and longitudinal forces from "in-tire" acceleration measurements. Specifically, we proposed an innovative set of sensors and regressors, based on the measurement of both standard vehicle sensors (wheel encoders) and accelerometers mounted directly in the tire.

Such estimates are based on the idea of extracting information from the phase shift between the wheel hub and the tire, which is due to the transmission of traction and braking forces exerted on the tire itself. We have described the whole data analysis

process, highlighting the filtering issues, discussing the spurious effects acting on the estimated signals, and motivating the signal processing procedures.

The scope of the work presented herein was to demonstrate the feasibility of the estimation method, using a simplified experimental setup. This scope is consistent with the present stage of development of smart tires.

Because only road tests have been performed (no test rig was available), no direct measurement of the "real" contact forces has been made. Hence, no direct comparison between "estimated" and "actual" forces is provided. However, as already said, today the key issue in contact-force estimation via smart tires is still the choice of the input variables ("regressors") used for force estimation. The sensor/regressor choice proposed and tested in this work is an important contribution in this research field at its present stage of development.

Needless to say, in order to move towards an industrial application of this idea, much more experimental testing should be done, both on the car and on the test bench, in many different driving situations and road conditions (higher speed, curve conditions, low-grip surface, etc.). This however goes beyond the scope and budget of this research work.

ACKNOWLEDGMENT

The authors would like to thank Ing. G. Wurzinger, for his constant help during this work.

REFERENCES

[1] E. Bakker, H. B. Pacejka, and L. Lidner, "A new tire model with an application in vehicle dynamics studies," *SAE Trans.*, pp. 83–93, 1989, paper 890087.

[2] E. Bakker, L. Nyborg, and H. B. Pacejka, "Tire modeling for use in vehicle dynamics studies," *SAE Trans.*, 1987, paper 870421.

[3] R. Bosch Gmbh, *Automotive Handbook*, 5th ed. Troy, MI: Society of Automotive Engineers, 2000.

[4] B. Breuer, U. Eichorn, and J. Roth, "Measurement of tyre-road friction ahead of the car and inside the tyre," in *Proc. Int. Symp. Adv. Veh. Control*, 1992, pp. 347–353.

[5] Bridgestone/Firestone, Inc., "Method of monitoring conditions of vehicle tires and tires containing a monitoring device therein," U.S. Patent 5 573 611, 1996.

[6] V. Cossalter, "Motorcycle dynamics," in *Race Dynamics*. Greendale, WI: Race Dynamics, 2002.

[7] U. Eichorn and J. Roth, "Prediction and monitoring of tire-road friction," in *Proc. 20th FISITA World Congr.*, Montreal, QC, Canada, 1992, pp. 67–74.

[8] F. Gustafsson, "Slip-based tire-road friction estimation," *Automatica*, vol. 33, no. 6, pp. 1087–1099, 1997.

[9] J. Hakanen, "Second-generation TPMS," *Tire Technol. Int.*, vol. 2004, pp. 60–62, 2004.

[10] U. Kiencke and L. Nielsen, *Automotive Control Systems for Engine, Driveline, and Vehicle*. Berlin, Germany: Springer-Verlag, 2000.

[11] R. Lot, "A motorcycle tire model for dynamic simulations: Theoretical and experimental aspects," *Meccanica*, vol. 39, no. 3, pp. 207–220, 2004.

[12] F. Mancosu, "Data from 'tire as a full system' to be used in the vehicle," presented at the Tire Technol. Conf., Cologne, Germany, Feb. 22–24, 2005.

[13] E. Ono, K. Asano, M. Sugai, S. Ito, M. Yamamoto, M. Sawada, and Y. Yasui, "Estimation of automotive tire force characteristics using wheel velocity," *Control Eng. Practice*, vol. 11, pp. 1361–1370, 2003.

[14] H. B. Pacejka, *Tire and Vehicle Dynamics*. Oxford, U.K.: Society of Automotive Engineers/Butterworth-Heinemann, 2002.

[15] W. R. Patserkamp and H. B. Pacejka, "The tire as a sensor to estimate friction," *Veh. Syst. Dyn.*, vol. 27, pp. 409–422, 1997.

[16] P. Pneumatici, "Method and system for controlling the behavior of a vehicle by controlling its tires," European Patent 1202 867B1, 2004.

[17] B. J. Quinn and M. Fernandes, "A fast technique for the estimation of frequency," *Biometrika*, vol. 78, no. 3, pp. 489–497, 1991.

[18] L. R. Ray, "Nonlinear state and tire force estimation for advanced vehicle control," *IEEE Trans. Control Syst. Technol.*, vol. 3, no. 1, pp. 117–124, Mar. 1995.

[19] L. R. Ray, "Nonlinear tire force estimation and road friction identification: Simulation and experiments," *Automatica*, vol. 33, no. 10, pp. 1819–1833, 1997.

[20] S. M. Savaresi, S. Bittanti, and H. C. So, "Closed-form unbiased frequency estimation of a noisy sinusoid using notch filters," *IEEE Trans. Autom. Control*, vol. 48, no. 7, pp. 1285–1292, Jul. 2003.

[21] S. M. Savaresi, S. Bittanti, and M. Montiglio, "Identification of semi-physical and black-box non-linear models: The case of MR-dampers for vehicles control," *Automatica*, vol. 41, pp. 113–117, 2005.

[22] S. M. Savaresi, M. Tanelli, and C. Cantoni, "Mixed slip-deceleration control in automotive braking systems," *ASME Trans./J. Dyn. Syst. Meas. Control*, vol. 129, no. 1, pp. 20–31, 2007.

[23] E. Silani, S. M. Savaresi, S. Bittanti, A. Visconti, and F. Farachi, "The concept of performance-oriented yaw-control systems: Vehicle model and analysis," *SAE Trans./J. Passenger Cars—Mech. Syst.*, pp. 1808–1818, 2003.

[24] E. Silani, S. M. Savaresi, S. Bittanti, D. Fischer, and R. Isermann, "Managing information redundancy for the design of fault-tolerant slow-active controlled suspension," *Tire Technol. Int.*, vol. 2004, pp. 128–133, 2004.

[25] M. Tanelli and S. M. Savaresi, "Friction-curve peak detection by wheel-deceleration measurements," in *Proc. IEEE Conf. Intell. Transport. Syst.*, Toronto, ON, Canada, 2006, pp. 1592–1597.

[26] R. A. Williams, "Tires for active chassis technology," presented at the Tire Technol Conf., Cologne, Germany, Feb. 22–24, 2005.